Chapter 2

Related Literature And Preliminaries

Image dehazing is the process of removing or reducing the amount of haze in an image. This process typically involves modifying the colors of pixels in an image in order to make the image appear clearer and more vibrant. Common techniques for image dehazing include contrast adjustment, color compensation, and image sharpening concept. This chapter presents the state-of-the-art works, background and preliminaries related to image dehazing. The experimental set-up, datasets, and relevant quantification metrics used in this dissertation are also discussed at the end of this chapter.

2.1 Related work on Image Dehazing

The image dehazing techniques can be classified into five categories: (i) Image enhancement-based, (ii) Image restoration-based, (iii) Image fusion-based, (iv) Deep

learning-based, (v) Edge-preserving filters-based as shown in Figure 2.1.

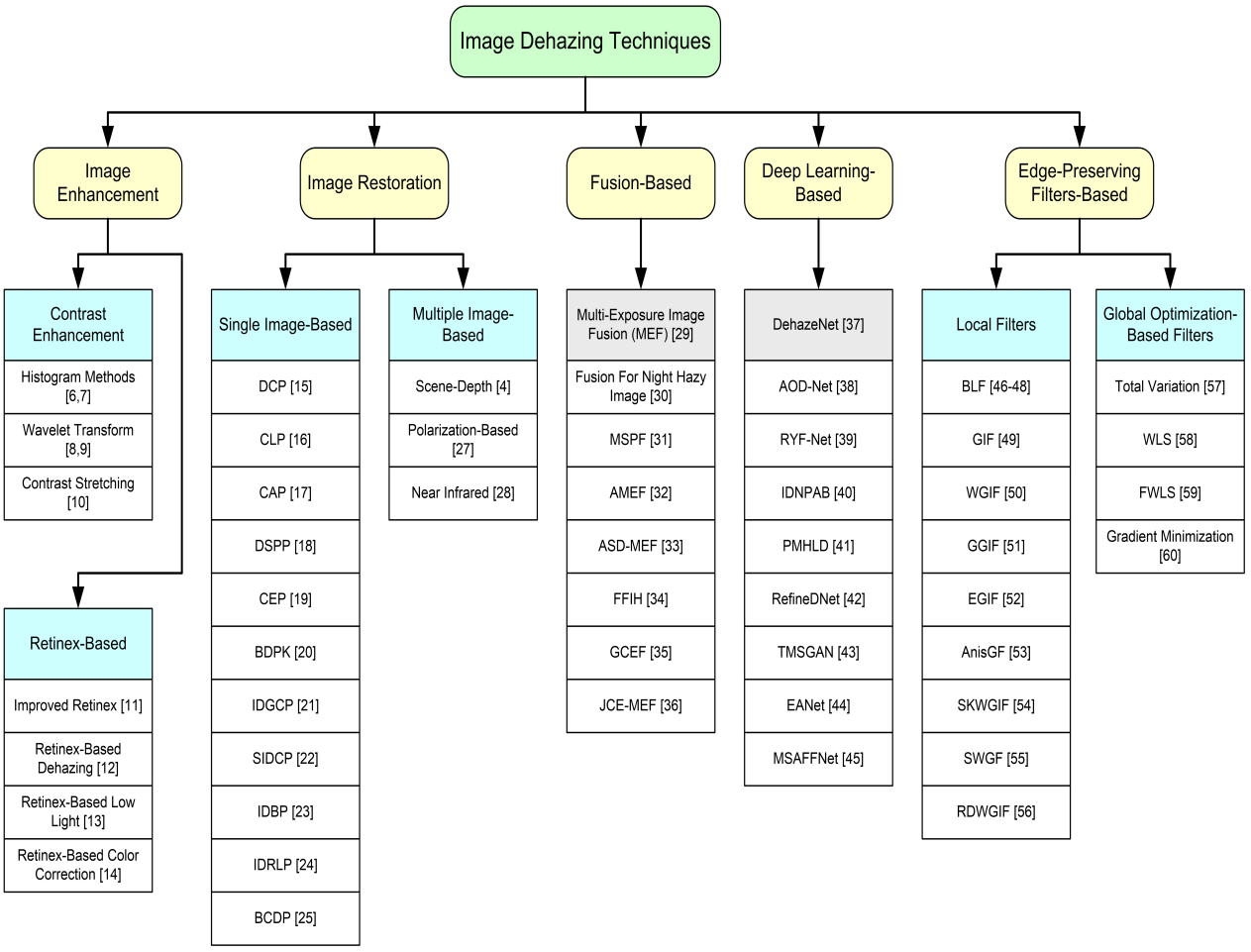

FIGURE 2.1: Taxonomy of image dehazing methods.

2.1.1 Image Enhancement-Based Dehazing

The image enhancement-based haze removal algorithms are further classified into two categories: contrast enhancement-based and retinex-based image dehazing.

2.1.1.1 Contrast Enhancement-Based Dehazing

The contrast enhancement algorithms can be based on enhancement in spatial domain or in frequency domaing. Image dehazing involves contrast enhancement techniques like histogram equalization [6, 7], wavelet transform [8, 9] or contrast stretching [10] to reduce the visible haziness on an image. These methods manipulate the contrast of the image to reveal details that might otherwise be obscured by the presence of haze. This improve image clarity and reduce visual artifacts that are caused by the presence of haze. These techniques can be used to effectively reduce the effects of haze, fog, mist, smog and other atmospheric visual obstructions.

2.1.1.2 Retinex-Based Image Dehazing

The retinex theory is widely used in digital photography, computer vision and image processing to reduce haze and maintain local contrast in an image. Retinex-based methods [11–14] are extensively use color correction and low-light image enhancement concept for image dehazing. Retinex theory uses a color constancy concept to maintain both the local contrast and haze removal process in image. More specifically, retinex theory describes a color imaging process in which images are processed to reveal finer details and more accurate color reproduction. The theory assumes that the observed luminosity of a scene comes from both direct light reflected from the scene and a separate light source, typically from the sky. The retinex theory combines these two inputs with an algorithm to improve the contrast of an image, as well as to increase color accuracy of the dehazed image.

2.1.2 Image Restoration-Based Dehazing

Image restoration is the process of restoring the degraded or corrupted image to its original form. This is done by using a variety of techniques and well-known physical model or prior knowledge. This technique improve the visual quality of the dehazed image. There are two kinds of image restoration-based dehazing methods: single image dehazing and multiple image dehazing methods.

2.1.2.1 Single Image-Based Dehazing

Single image dehazing is an approach to reduce the amount of haze from a single input image. It focuses on removing the visible effects of haze, such as contrast reduction, color distortion, and blur. It involves techniques like extraction of dark channel, color transform, atmospheric light estimation, and transmission light estimation. Various prior-knowledge based algorithms are in existence for single image dehazing. The prior-knowledge based well-known haze removal methods are dark channel prior (DCP) [15], color line prior (CLP) [16], color attenuation prior (CAP) [17], difference-structure-preservation prior (DSPP) [18], color ellipsoid prior (CEP) [19], Bayesian dehazing prior knowledge (BDPK) [20], gamma correction prior-based image dehazing IDGCP [21], saturation based iterative dark channel prior (SIDCP) [22], blended prior-based image dehazing (IDBP) [23], region line prior based image dehazing (IDRLP) [24], bounded channel difference prior (BCDP) [25] etc.

A novel dark channel prior (DCP) method is presented in [15] for single image dehazing. DCP is a well-known haze removal algorithm. It removes haze from single input image. It is based on the assumption that the most common element found in a hazy image is the presence of a homogeneous, bright sky in the background of

the image, which is referred to as the dark channel. The basic idea is to remove this dark channel by enhancing the image contrast and colors to restore better visibility of the scene. Here, main steps include calculating the dark channel by selecting a certain number of pixels from a patch, estimating the global atmospheric light [26] from the brightest pixels in the dark channel, and finally, reconstructing the original image by a modified global atmospheric scattering model. However, due to local linear filtering it generates halos at depth discontinuities. This method is computationally inefficient and often fails in large sky regions or bright objects.

A color line prior (CLP) based algorithm is presented in [16] for single image dehazing. In this work, color lines are fitted in RGB space per-patch and restoring the scene by small patches with constant transmission. However, due to additive haze component, color lines do not pass through the origin accurately. Due to this, halos and color veil persist in the restored image. Next, a linear model-based color attenuation prior (CAP) algorithm is presented in [17] for single image dehazing. This work used statistical rules from large number of hazy images to restore the haze free image. It removes haze efficiently. However, due to non constant of scattering coefficient in the homogeneous atmospheric conditions, it estimates atmospheric light inaccurately.

In [18], a difference structure preservation prior (DSPP) model is developed to remove haze from single input image. It estimates the optimal transmission map frequently and restores the haze-free image. Then, a novel image dehazing algorithm based on color ellipsoid prior (CEP) is presented in [19]. In CEP, an optical model and boundary prior are used to estimate and recast the transmission map, respectively. In [20], a novel Bayesian probabilistic algorithm is proposed for single image dehazing. This work modelled with factorial Markov random field [5] in

which the scene albedo and depth value, both statistically independent layers, are estimated jointly. It removes dense haze efficiently. However, over-saturation and unnatural distortion persists in the restored image.

In the continuation, a gamma correction prior IDGCP based haze removal algorithm is presented in [21]. It synthesizes a virtual transformation of input hazy image and removes haze globally by extracting the depth information. Next, saturation based iterative algorithm (SIDCP) approach is used in [22] for image haze removal. In this work, dark channel is reformulated in saturation and brightness terms and transmission map is estimated without computing the dark channel. A novel blended prior model is proposed in [23] for image dehazing. This method has two modules such as atmospheric light estimation (ALE) and a multiple prior constraint (MPC) based effective image dehazing method. Recently, region line prior (RLP) and bounded channel difference prior (BCDP) based haze removal methods are presented in [24], [25], respectively. They remove haze efficiently and preserve edge information precisely in layers.

2.1.2.2 Multiple Image-Based Dehazing

Multiple image dehazing is an approach to reduce the amount of haze from multiple images simultaneously. This approach is based on extracting the common features from the multiple hazy images, and then using them to reconstruct the clarity of each of the images. This approach reduces the amount of haze in each of the images more effectively than a single image dehazing approach. The multiple image dehazing based algorithms are scene depth [4], polarization based [27], and near-infrared [28]. In [4], different weather conditions and color variations of the scene are computed for image dehazing. However, due to fixed atmospheric scattering, halos persist in

the restored image. Polarization is a challenging task to decide the haze effect. In [27], polarization is used to remove haze in images based on the effects of scattering on light polarization. However, halos persist due to unpolarized atmospheric light. In [28], near-infrared images (captured from near-infrared camera) are transformed into scene depth for image dehazing. The main drawback of this work is that it dehaze image without atmospheric scattering model and due to that halos and color cast persist in the result.

2.1.3 Image Fusion-Based Dehazing

In fusion-based techniques, multiple derivatives of single input image or multiple input images are used to get dehazed image. The main aim of fusion techniques is to generate a haze-free image by combining the complementary of the single input image. A novel multi-scale fusion algorithm is presented in [29] for efficient haze removal. In [29], two derivatives of single input hazy image are combined with three weight-maps to get haze free image as output. Further, a fusion based algorithm is developed in [30] for night time image dehazing. It works effectively for night time haze. However, over-smoothness persist in sharp regions. Then, a multi-scale pyramid fusion algorithm by using some haze relevant features is presented in [31] for effective haze removal. In [32], an artificial multiple-exposure image fusion algorithm is developed for image dehazing. Scene-depth estimation as well as transmission map refinement process are not required in this method. Next, an adaptive structure decomposition integrated with multi-exposure image fusion is proposed in [33] to remove haze accurately. This method removes haze and improves visual quality of the restored image. After that, a fast fusion based algorithm with improved histogram and atmospheric map is used in [34] for efficient haze removal. The central concept of this work is to combine multi-scale fusion approach with prior

knowledge, thereby producing balanced image contrast enhancement and intrinsic color preservation accurately. A gamma-corrected underexposed fusion algorithm is presented in [35] to improve the performance and robustness of image dehazing. Recently, an efficient joint contrast enhancement and multi-exposure fusion framework is proposed in [36] for real-time image dehazing.

2.1.4 Deep Learning-Based Dehazing

Deep learning based methods have been used for image dehazing, image deblurring, and image super-resolution. Deep learning methods are more robust and advanced as compared to traditional methods. In addition, deep learning methods can learn from both the intrinsic and statistical properties of the data to produce more accurate and robust haze free images. They have been used to effectively dehaze multiple images at once. Recently, many deep learning based methods have been proposed to remove haze more efficiently than the state-of-the-art methods. Several deep learning based methods such as DehazeNet [37], AODNet [38], RYF-Net [39], IDNPAB [40], PMHLD [41], RefineDNet [42], TMSGAN [43], EANet [44], MSAFFNet [45] are developed to improve the efficiency and the visual quality of the dehazed images.

A convolutional neural network (CNN) called DehazeNet was proposed for single image dehazing [37]. This method used CNNs to learn a non-linear mapping from the hazy image **I** to a clear image **J**. The network was trained with a large dataset of hazy images and used to predict the transmission map and the optical depth. These were then used to estimate the atmospheric light and compute the dehazed image. Next, all in one dehazing network (AOD-Net) is presented in [38]. This network uses a light-weight CNN framework to generate haze free image directly without estimating the atmospheric and transmission light separately. Further, a

CNN based deep architecture is presented in [39]. It estimates transmission map more efficiently and remove haze strongly. This network considers hazy image as a input and extracts relevant features for image dehazing. Next, an end-to-end network with parallel spatial- and channel- wise attention block (IDNPAB) is presented in [40] for image dehazing. Then, a patch-map based hybrid learning dehazing (PMHLD) technique with bi-attentive generative adversarial network is presented in [41] for image dehazing. A two-stage weakly supervised framework-based haze removal algorithm is presented in [42]. In this work, a prior based and learning based two approaches are combined and dehazed model is divided into two subtasks. These tasks improve the visibility restoration and realness of dehazed image. Recently, a multi-scale generative adversarial network (TMS-GAN) with haze generation (HgGAN) and haze removal (HrGAN) model is developed in [43] for efficient haze removal. An edge-aware network with edge features and contextual features is presented in [44] for image dehazing. A compact multi-scale attention feature fusion network (MSAFFNet) [45] is proposed using channel attention and a multi-scale spatial attention module for image dehazing.

2.1.5 Edge-preserving Filtering-Based Dehazing

Edge-preserving filtering based single image dehazing is a technique that is used to remove haze from digital images. The edge-preserving filters preserve edges in the output image while the details in the input image removed. All the edge-preserving filters can be further separated into two categories: local-linear transform model based algorithms and global optimization based algorithms. The bilateral filter (BLF) [46–48], guided image filter (GIF) [49], and its extension weighted guided image filter (WGIF) [50], gradient domain guided image filter (GGIF) [51], effective

guided image filter (EGIF) [52], anisotropic guided image filter (AnisGF) [53], steering kernel-based weighted guided image filter (SKWGIF) [54], side window guided filter (SWGF) [55], and robust double weighted guided image filter (RDWGIF) [56], etc. are local linear transform model based edge-preserving filters.

Some of the global optimization-based algorithms are total variation-based filter [57], its extension weighted least squares (WLS) [58], fast weighted least squares (FWLS) [59] and L_o gradient minimization algorithm [60]. The global optimization based filters always provide more adequate results than the local edge-preserving filters. They remove halos, over-smoothing, and color distortions accurately and preserve edge information precisely in hazy regions. However, due to high computational cost, and iterative nature they require large execution time.

The local edge-preserving filters generally have high efficiency, but the resultant image may get affected with halos and usually fail to preserve edge information in sharp regions. A novel guided image filter (GIF) is presented in [49]. In GIF [49], a local linear model is used to represent filtered output with the help of a guided image. This method reduces halos, gradient reversal artifacts and preserves edge information more accurately than the existing [46–48] methods. However, it fails to preserve edge-information in sharp region. Next, Li *et al.* proposed a weighted guided image filter (WGIF) in [50] to remove halos more accurately and preserve edge information precisely than BLF and GIF methods. In WGIF, an edge-aware weighting is introduced in the cost function of GIF [49] to remove the halos and preserve edge informations in the sharp regions. However, due to single-scale edge-aware weighting and fixed regularization parameter, over-smoothing effects persist in sharp regions. Further, an edge-preserving decomposition-based an effective single

image haze removal algorithm is presented in [61]. This method refines the transmission map by decomposing it into base layer and detail layer. However, halos and over-smoothing still persist in the sharp regions. Next, a gradient domain guided image filter (GGIF) is proposed in [51] to remove halos and over-smoothing strongly than GIF [49] and WGIF [50]. But, over-smoothing increases with increasing value of the regularization parameter in sharp regions. Next, an effective guided image filter (EGIF) based haze removal algorithm is proposed in [52]. This work averages the local variances of all pixels from input image and then incorporates it into the cost function of GIF to remove haze strongly and preserve edges accurately than the existing guided filters.

Next, an anisotropic guided filter (AnisGF) [53], steering kernel based- guided image filter (SKGIF) [62] and steering kernel based weighted guided image filter (SKWGIF) [54] are proposed to remove haze efficiently. However, due to local linear model, high computational complexity and fixed regularization parameter, halos and over-smoothing persist in the sharp regions. The non-local side window guided filter (SWGF) [55] is an advanced image processing technique that can be used to correct images corrupted by haze. This technique applies a guided image filter with a side window that reduces the influence of near-by regions. This filter uses a local side window to overcome the limitation of the original guided filter, which consider only the nearby regions in a two-dimensional space. Then, a robust double-weighted guided image filtering (RDWGIF) is proposed in [56] to remove halos and preserve edge information in sharp regions efficiently. This filter is proposed by incorporating a robust edge-aware weighting (REAW) and the mollifier from Sobolev space theory into the cost function of the GIF.

2.1.6 Background on Edge-Preserving Filtering

2.1.6.1 Guided Image Filtering (GIF)

The guided image filter (GIF) [49] is local linear optimization based an edge-preserving smoothing filter. In this filter, a guidance image I and an input filtering image p are assumed to be similar for easy analysis. Further, it is assumed that the filtered output q is a linear transform of input guidance image I in the window $\omega_{\zeta_1}(k)$ and can be expressed as:

$$q_i = a_k I_i + b_k, \forall i \in \omega_{\zeta_1}(k), \tag{2.1}$$

where $\omega_{\zeta_1}(k)$ is a square window of radius ζ_1 centred at k^{th} pixel position. The parameters a_k and b_k are two constants in the square window $\omega_{\zeta_1}(k)$. The values of linear coefficients a_k and b_k are evaluated by minimizing the cost function $E(a_k, b_k)$ as given in linear ridge regression model [63, 64]:

$$E(a_k, b_k) = \sum_{i \in \omega_{\zeta_1}(k)} [(a_k I_i + b_k - p_i)^2 + \varepsilon a_k^2], \tag{2.2}$$

where p is an input filtering image and ε is a regularization parameter used to penalize large a_k value. The cost function in a square window ω of radius ζ_1 represents a linear ridge regression model [63, 64]. Its solution is obtained in terms of two optimized linear constants: a_k and b_k. They can be expressed as:

$$a_k = \frac{\mu_{I \odot p,\ \zeta_1}(k) - \mu_{I,\ \zeta_1}(k)\mu_{p,\ \zeta_1}(k)}{\sigma^2_{I,\ \zeta_1}(k) + \varepsilon}, \tag{2.3}$$

and

$$b_k = \mu_{p,\ \zeta_1}(k) - a_k \mu_{I,\ \zeta_1}(k). \tag{2.4}$$

where $\odot$ is the element-wise multiplication of two matrix. $\mu_{I\odot p,\ \zeta_1}(k)$, $\mu_{I,\ \zeta_1}(k)$ and $\mu_{p,\ \zeta_1}(k)$ are the mean values of $I \odot p$, I and p in the window $\omega_{\zeta_1}(k)$, respectively. In GIF [49], ε determines criterion of edge information in flat as well as sharp regions by following two cases:

- Specifically, ε should be larger than $\sigma^2_{I,\ \zeta_1}(k)$ to preserve edges in smooth regions, and
- ε should be smaller than $\sigma^2_{I,\ \zeta_1}(k)$ to preserve edges in the sharp regions.

2.1.6.2 Weighted Guided Image Filtering (WGIF)

The GIF is a local optimization based effective and the fastest edge-preserving filter. It removes halo artifacts and the gradient reversal artifacts from the flat regions. However, halo artifacts are visible in the sharp regions due to fixed regularization parameter (ε). To overcome this drawback, an edge-aware weighting based guided image filter (WGIF) was proposed in [50]. Similar to GIF [49], the values of linear coefficients a_k and b_k are evaluated by minimizing the cost function $E(a_k, b_k)$ as given in linear ridge regression model [63, 64]:

$$E(a_k, b_k) = \sum_{i \in \omega_{\zeta_1}(k)} [(a_k I_{\mathrm{i}} + b_k - p_i)^2 + \frac{\varepsilon a_k^2}{\Gamma_I(k)}], \tag{2.5}$$

where $\Gamma_I(k)$ represents the edge-aware weighting of WGIF and can be evaluated by local variances of 3×3 windows of all pixels as follows:

$$\Gamma_I(k) = \frac{1}{N} \sum_{i=1}^{N} \frac{{\sigma^2}_{I,\ 1}(k) + \lambda}{{\sigma^2}_{I,\ 1}(i) + \lambda}, \tag{2.6}$$

where ${\sigma^2}_{I,\,1}(k)$ is the local variance of I in $\omega_{\zeta_1}(k)$. Here, λ is a small positive constant calculated by the expression $(0.001 \times M)^2$ for M intensity range of image. The optimum value of linear constants can be expressed as:

$$a_k = \frac{\mu_{I \odot p,\,\zeta_1}(k) - \mu_{I,\,\zeta_1}(k)\mu_{p,\,\zeta_1}(k){\sigma^2}_{I,\,\zeta_1}(k) + \frac{\varepsilon}{\Gamma_I(k)}}{{\sigma^2}_{I,\,\zeta_1}(k) + \frac{\varepsilon}{\Gamma_I(k)}}, \tag{2.7}$$

$$b_k = \mu_{p,\,\zeta_1}(k) - a_k\mu_{I,\,\zeta_1}(k). \tag{2.8}$$

The WGIF removes halo artifacts and preserves edge information more precisely than GIF [49]. However, over smoothing increases with increase in the regularization parameter in both regions of image. It is due to single scale edge-aware weighting and fixed ε value in WGIF [50].

2.1.6.3 Gradient-Domain Guided Image Filter (GGIF)

Next, a novel multi-scale edge-aware weighting based gradient domain guided image filter (GGIF) [51] is proposed using local variances of 3×3 and $(2\zeta_1 + 1) \times (2\zeta_1 + 1)$ window sizes for all pixels of image. In the GGIF [51], the local variance in WGIF [50] is replaced by a new edge-aware weighting $\hat{\Gamma}_I(k)$. It can be expressed as:

$$\hat{\Gamma}_I(k) = \frac{1}{N}\sum_{i=1}^{N}\frac{|G(k)| + \lambda}{|G(i)| + \lambda}, \tag{2.9}$$

where $G(k) = \sigma_{I,1}(k)\sigma_{I,\,\zeta_1}(k)$ and $G(i) = \sigma_{I,1}(i)\sigma_{I,\,\zeta_1}(i)$ can be computed at k and i pixel positions, respectively while N represents the number of pixels in the $\omega_{\zeta_1}(k)$ window.

Similar to GIF [49] and WGIF [50] the values of linear coefficients a_k and b_k are evaluated by minimizing the cost function $E(a_k, b_k)$ as given in linear ridge regression

model [63, 64]:

$$E(a_k, b_k) = \sum_{i \in \omega_{\zeta_1}(k)} [(a_k I_{\mathrm{i}} + b_k - p_i)^2 + \frac{\varepsilon \{a_k - \gamma_k\}^2}{\hat{\Gamma}_I(k)}], \tag{2.10}$$

where γ_k defined as an edge-aware smoothing parameter for regulating a_k in the cost function and

$$\gamma_k = 1 - \frac{1}{1 + exp^{\eta(G(k) - \mu_{G,\infty})}}, \tag{2.11}$$

where $\mu_{G,\infty}$ represents the mean (average) value of all $G(i)$ and η can be expressed as:

$$\eta = \frac{4}{\mu_{G,\infty} - min(G(i))}. \tag{2.12}$$

The optimum value of a_k and b_k can be calculated by the following expression:

$$a_k = \frac{\mu_{I \odot p,\ \zeta_1}(k) - \mu_{I,\ \zeta_1}(k)\ \mu_{p,\ \zeta_1}(k) + \frac{\varepsilon \gamma_k}{\hat{\Gamma}_I(k)}}{{\sigma^2}_{I,\ \zeta_1}(k) + \frac{\varepsilon}{\hat{\Gamma}_I(k)}}, \tag{2.13}$$

$$b_k = \mu_{p,\ \zeta_1}(k) - a_k \mu_{I,\ \zeta_1}(k), \tag{2.14}$$

where $\mu_{I \odot p}$ represents mean value of $(I \odot p)$.

2.1.6.4 Effective Guided Image Filter (EGIF)

An effective guided image filter (EGIF) is proposed in [52] for contrast enhancement. In this filtering, average of local variances for all pixels in a window $\omega_{\zeta_1}(k)$ is used to design the new edge-aware weighting. It can be expressed as:

$$\overline{\Gamma}_I(k) = \overline{\sigma}^2 = \frac{1}{N} \sum_{k=1}^{N} {\sigma^2}_{I,\ 1}(k). \tag{2.15}$$

where $\sigma^2_{I,1}$ is the local variance I in window $\omega_{\zeta_1}(k)$ and $\overline{\sigma}^2$ is average of local variances for all pixels. To determine the linear coefficient a_k and b_k, cost function in EGIF is minimized by linear ridge regression model [63, 64]. The values of linear coefficients a_k and b_k are evaluated by minimizing the cost function $E(a_k, b_k)$ as:

$$E(a_k, b_k) = \sum_{i \in \omega_k} \left((a_k I_i + b_k - p_i)^2 + \varepsilon \overline{\Gamma} a_k^2 \right). \tag{2.16}$$

The optimal value of linear coefficients a_k and b_k can be obtained by solving the cost function in 2.16. They can be expressed as:

$$a_k = \frac{\frac{1}{|\omega|} \sum_{i \in \omega_k} I_i p_i - \mu_k \bar{p}_k}{\sigma_k^2 + \varepsilon \overline{\Gamma}}, \tag{2.17}$$

and

$$b_k = \bar{p}_k - a_k \mu_k. \tag{2.18}$$

2.2 Experimental Set-Up and Image Datasets

The entire experimentation and comparative evaluation are performed on Matlab R2018a on a PC with Intel (R) Core (TM) i7-6700 CPU @ 3.40 GHz of a 64-bit operating system with RAM-8GB.

2.2.1 Dataset

The performance of the proposed algorithms are tested on indoor/outdoor synthetic hazy, indoor/outdoor real-time hazy, dense hazy, synthetic textures, underwater hazy and night-time hazy image datasets, viz. **Fattal** [16], **D-HAZY** [65], **NYU**

[66], **NYU2** [66], **FRIDA** [67], **Middlebury** [68], **Haze-RD** [69], **I-HAZE** [70], **O-HAZE** [71] **NH-HAZE** [72], **RESIDE-ITS** [73], **RESIDE-OTS** [73], **RESIDE-SOTS** [73], **RESIDE-RTTS** [73], **RESIDE-HSTS** [73], **Dense hazy images** [74], **synthetic textures** [75], **underwater hazy images** [76], **Image-Net** [77], **Night-time hazy** [78].

2.3 Performance Evaluation Metrics

Following performance metrics are usually used to assess the effectiveness of the proposed methods and the existing haze removal methods. Generally, the quantitative metrics can be categorized based on referenced and non-referenced methods. The non-referenced based performance metrics refer to performance metrics which are determined independently without comparison to an external or objective reference and referenced based performance metrics evaluate the performance of an image by comparing it to a reference image. The non-referenced performance metrics are contrast enhancement e [79], $\overline{r}$ [79], $\overline{\alpha}$ [79], visual contrast measurement (VCM) [80], fog aware density evaluator (FADE) [81], color natural index (CNI) [82], blind image quality index (BIQI) [83], and natural image quality evaluator metric (NIQE) [84]. The contrast gain C_{g} [85], structural similarity index (SSIM) [86], peak to signal noise ratio (PSNR) [87], edge keeping index (EKI) [88], color difference metric (CIEDE2000) [89], and universal image quality index (UIQI) [90] are referenced performance metrics.

2.3.1 Contrast Enhancement Metric e:

The performance metric e [79] denotes the capability of restoring edges. It evaluates the newly visible edges after restoration. Its higher value signifies superior restoration efficacy. It can be expressed as:

$$e = \left\{ \frac{n_r - n_o}{n_o} \right\} \times 100, \tag{2.19}$$

where n_r and n_o denote the total number of visible edges in the restored- and in the original- image, respectively.

2.3.2 Contrast Enhancement Metric $\overline{r}$:

The $\overline{r}$ metric [79] is used to assess the average visibility enhancement. It calculates the mean ratio of gradients at the visible edges. Its higher value indicates better restoration capability. It can be expressed as:

$$\overline{r} = exp\left[\frac{1}{n_r} \sum_{x_i \in \delta} log\ r_i \right], \tag{2.20}$$

where x_i represents the pixel at i^{th} position on the visible edge of the restored image and δ represents the sets of these pixels while r_i represents the ratio of the gradient at x_i in the restored image to the gradient at x_i in the input image.

2.3.3 Contrast Enhancement Metric $\overline{\alpha}$:

The enhancement metric $\overline{\alpha}$ [79] denotes the percentage of saturated white or black pixels on the visible edges of the restored image. It can be expressed as:

$$\overline{\alpha} = \frac{N_s}{N} \times 100. \tag{2.21}$$

where N_s represents the number of saturated pixels (pixels that become completely black or white) after dehazing and N represents the total number of pixels present in the image. The small value of $\overline{\alpha}$ represents better restoration result.

2.3.4 Visual Contrast Measurement (VCM):

The visual contrast measurement (VCM) [80] parameter evaluates the quality of the restored image. The large VCM value indicates the better visibility of the recovered image.

2.3.5 Fog Aware Density Evaluator (FADE):

The perceptual fog aware density evaluator (FADE) computes the visibility of the restored image [81]. The smaller value of FADE indicates the lower haze concentration of dehazed result

2.3.6 Colour Natural Index (CNI):

The color natural index (CNI) [82] metric computes the fidelity and naturalness of the restored image. It can be expressed as:

$$N_{image} = \frac{n_{skin} * N_{skin} + n_{grass} * N_{grass} + n_{sky} * N_{sky}}{n_{skin} + n_{grass} + n_{sky}}. \tag{2.22}$$

where n_{skin}, n_{grass} and n_{sky} represents three different types of pixels, whereas N_{skin}, N_{grass} and N_{sky} denote the CNI values of three different types of pixels. The range of CNI is [0∼1] [82]. The restored image is more natural, if CNI value is close to 1.

2.3.7 Image Quality Index (BIQI):

The blind image quality index (BIQI) [83] is a no reference metric. In this metric, natural scene statistic (NSS) model is used to calculate the distorted image. It is expressed as:

$$BIQI = \sum_{i=1}^{5} p_i \ . \ q_i, \tag{2.23}$$

where p_i and q_i are probability and quality of each score distortion, respectively. The lower BIQI score denotes better outcomes.

2.3.8 Natural Image Quality Index (NIQE):

The natural image quality evaluator metric [84] is a blind or no reference image quality (NR-IQA) metric. A smaller NIQE represents that the restored image is more realistic and natural.

2.3.9 Contrast Gain C_g:

The contrast gain C_{g} [85] measures contrast of the restored image. Its larger value indicates the higher contrast of the dehazed image. The contrast gain C_g [85] is defined as the average contrast difference between hazy and haze-free image. Its higher value indicates that how efficiently the given haze removal method dehaze the input image. It can be expressed as:

$$C_g = (C_{avg})_{HF} - (C_{avg})_{HZ}. \tag{2.24}$$

where $(C_{avg})_{HF}$ and $(C_{avg})_{HZ}$ are represent average contrast value of haze free image and average contrast value of hazy image, respectively.

2.3.10 Structural Similarity Index (SSIM):

The SSIM metric [86] quantify the image quality degradation by comparing the reference image with the processed image. The range of SSIM is [-1, 1]. The restored image is identical to the reference image when SSIM equal to 1. It is expressed as:

$$SSIM = F(L_c, C_c, S_c). \tag{2.25}$$

where L_c, C_c and S_c represent the luminance-, contrast- and saturation- comparison, respectively.

2.3.11 Peak Signal to Noise Ratio (PSNR):

The PSNR metric [87] is expressed as:

$$PSNR = 10 * log\{\frac{f_{max}^2}{MSE}\}, \tag{2.26}$$

where f_{max} is the maximum grey level (255 for 8-bit image). The mean squared error (MSE) evaluated from the original and the restored image. It is written as:

$$MSE = \frac{1}{m \times n} \sum_{i=0}^{m-1} \sum_{j=0}^{n-1} [f_o(i,j) - f_r(i,j)]^2. \tag{2.27}$$

where $m \times n$ represent the size of the image. The f_o and f_r are the original and the restored image, respectively.

2.3.12 Edge-Keeping Index (EKI):

The edge keeping index (EKI) [88] metric is used to represent the closeness of edge information near flat or sharp regions in the recovered image with reference to the input hazy image.

2.3.13 CIEDE2000:

The CIEDE2000 metric [89] is used to measure the color difference between the restored and the ground truth images. In this metric, color difference loss C_{Loss} is calculated as follows:

$$C_{Loss} = \frac{1}{N} \sum_{i}^{N} C_{Diff}(G_i, R_i). \tag{2.28}$$

where N represents the total number of pixels present in the image, C_{Diff} is the color difference of each pixel between ground truth image G_I and the restored image R_I, respectively. The range of CIEDE2000 is [0, 100]. The smaller value indicates lower color loss.

2.3.14 Universal Image Quality Index (UIQI):

The universal image quality index (UIQI) [90] metric has combination of three components viz. correlation coefficient, luminance distortion and contrast distortion. It can be expressed as:

$$Q_{index} = \frac{4 * \sigma_{xy} * \overline{x}\ \overline{y}}{[({\sigma_x}^2 + {\sigma_y}^2) * \{(\overline{x})^2 + (\overline{y})^2\}]} \times 100. \tag{2.29}$$

where x and y represent the original and the restored image signals, respectively while σ_x^2 and σ_y^2 are the variance of the original and the restored image, respectively. It ranges from [-1, 1]. When the restored image is identical to the original image, maximum value 1 is achieved.

2.4 Concluding Remarks

In this Chapter, we discussed various haze removal techniques using image enhancement, image restoration, fusion based, deep learning based and edge-preserving filters. The local optimization based edge-preserving guided image filter (GIF), weighted guided image filter (WGIF), gradient domain guided image filter (GGIF), and effective guided image filter (EGIF) are discussed in detail in the background section. The specifications of edge-aware weighting constraint, regularization parameter ε, and window radius ζ_1 are introduced. The performance of haze removal

algorithms is dependent on the nature of the images used. So, the performance of these algorithms must be tested on various datasets. We evaluated our proposed algorithms on several datasets. A brief introduction about the datasets used in our work is also covered in this Chapter. Next, experimental set-up, relevant non-referenced quantification metrics like e, $\overline{r}$, $\overline{\alpha}$, visual contrast measurement (VCM), fog aware density evaluator (FADE), color natural index (CNI), blind image quality index (BIQI), natural image quality evaluator metric (NIQE), and referenced quantification metrics like contrast gain C_{g}, structural similarity index (SSIM), peak to signal noise ratio (PSNR), edge keeping index (EKI), color difference metric (CIEDE2000), and universal image quality index (UIQI) are introduced and their details are discussed.